Functional Materials 13, No.2 (2006)

Electrically induced spectral and spatial instabilities of photoresponse CdZnTe crystals

V.P.Mygal, A.S.Phomin

N.Zhukovsky National Aerospace University "KhAI",
17 Chkalov St., 61070 Kharkiv, Ukraine

Received November 2, 2005

The features of $I = f(\lambda)$ and $I = f(x)$ dependences in $Cd_{1-x}Zn_xTe$ crystals containing a variety of two-dimensional structural defects, which become manifested under simultaneous action of biasing and modulating fields, have been exposed and explored. Basing on comparison of spectral and coordinate photocurrent dependences and their wavelet-spectrograms obtained at appropriate polarity, frequency, and on-off time ratio characteristics of the modulating square pulse voltage, an relation has been found between certain wavelength ranges of spectral instability and coordinates of structural defects aggregates originating those waves.

Выявлены и исследованы особенности зависимостей $I = f(\lambda)$ и $I = f(x)$ кристаллов $Cd_{1-x}Zn_xTe$, содержащих двумерные дефекты структуры, которые проявляются при одновременном воздействии смещающего и модулирующего полей. На основе сопоставления спектральных и координатных зависимостей фототока и их вейвлет-спектрограмм, полученных при соответствующих полярности, частоте и скважности модулирующего П-образного напряжения, установлена связь между определенными диапазонами длин волн спектральной неустойчивости и координатами порождающих их ансамблей дефектов структуры.

A variety of two-dimensional structural defects is a feature of $Cd_{1-x}Zn_xTe$ crystals. Some aggregates of the two-dimensional structural defects (2DSD) are among the main factors limiting the wide usage of the crystals as ionizing radiation sensors [1]. The 2DSD aggregates cause a low useable material yield in crystalline boule (20 to 30 %) and essential difficulties in manufacture of detectors with the working element volume exceeding 1 cm^3 [1, 2]. The 2DSD influence on the photosensitivity spectrum is manifested itself as the response instability in certain spectral ranges [3, 4]. At the same time, it is difficult to identify the 2DSD which influence significantly the crystal electrophysical properties. Therefore, the main purpose of this study is a search for complementary detection methods of 2DSD aggregates causing the photoresponse instability.

The spectral and coordinate photocurrent dependences were studied in $Cd_{1-x}Zn_xTe$ (x = 0.1 to 0.2) crystals with resistivity $\rho = 10^{10} \div 10^{11}$ $\Omega \cdot$ cm. The crystals were grown by the High-Pressure Vertical Bridgman (HPVB) method in various conditions. The 2DSD distribution character was studied by optical, dielectric, and acoustic methods [5]. The In–Ga and Au contacts were deposited onto the opposite largest faces of $11 \times 11 \times 2$ mm^3 size parallelepiped-shaped samples. The 2DSD were placed in parallel or perpendicular planes to the largest faces of the sample. The steady-state photocurrent spectra (PHC) and photocurrent dependences $I = f(x)$ on the position coordinate x of a monochromatic probe were measured in the biasing electrical field of $E_b = 10 \div 3 \cdot 10^2$ V/cm strength using an electrometric transducer on the basis of AD745 operational amplifier. The signal was converted to digital

form at a high sampling frequency of $10^4 \div 10^6$ kHz, thus providing reliable experimental data processing in the MATLAB software package. In some experiments, additional square-pulse modulating pulse voltage of positive or negative polarity with $U_{mod} = 10 \div 60$ V amplitude, 0.1÷30 kHz frequency and on-off time ratio n=20÷50 from a G5-60 generator was added to the bias field E_b. The crystal surface was scanned using a monochromatic optical probe of 50÷70 μm width by moving sample automatically at a speed of 0.5 to 10 mm/min. The dielectric crystal response was studied in 200 Hz to 10 kHz frequency range by means of measuring bridge converter with a separation system of polarization and dissipative components of dielectric response [6].

All studied samples that were cut out of ingots of 50 mm diameter were subdivided into two groups. The first group includes crystals that are most optically uniform and have relatively low density of structural defects, voids, and inclusions. The second group samples (cut out of the ingots grown at higher crystallization front curvature) contain various boundaries formed by two-dimensional (twins, blocks, slip bands, etc.) and other structural defects. Those samples, in turn, were subdivided into two types. The 2DSD were situated in parallel (type $II_{\parallel}$) and perpendicularly (type $II_{\perp}$) to the largest faces of the first type and second type samples, respectively. The photocurrent spectra of first group samples contain one peak reproducible well at repeated measurements. At the same time, the PHC spectra of all second group samples include a larger spectral region and show some fluctuations. In addition, the $I = f(\lambda)$ dependences for the of type $II_{\perp}$ samples contain additional peaks (Fig. 1, curve *2*) and also depend on direction and strength of the biasing field. Thus, electrostimulated photoconductivity is observed in such crystals [7]. Some of the observed peaks are reproduced poorly at repeated scanning of the photocurrent spectra. The photocurrent and photodielectric response spectra of second group samples contain a series of sections that differ in the photoresponse change rate and have fuzzy boundaries. Therefore, the decomposition method offered in [8] are unsuitable in this case. However, preliminary studies have shown that the wavelet analysis is an effective way to spectral dependences decomposition. The method makes it possible to distinct clearly the regions with

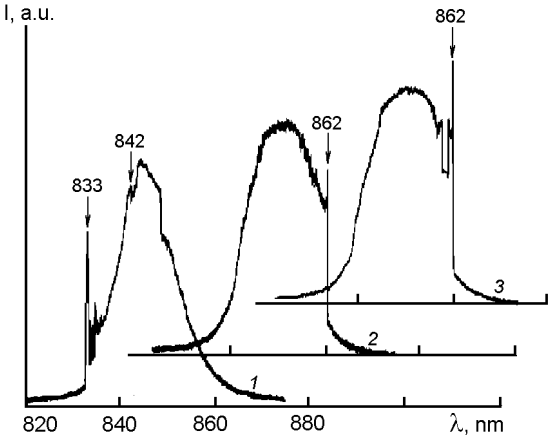

Fig. 1. Photocurrent spectra for the second-group $Cd_{0.9}Zn_{0.1}Te$ crystal of $II_{\perp}$ type: under simultaneous influence of biasing field E_b and modulating positive square pulse voltage U_{mod} at on-off time ratio n = 20 (*1*); under only biasing field E_b (*2*); under simultaneous influence of biasing field E_b and modulating negative square pulse voltage U_{mod} at on-off time ratio $n = 15$ (*3*). For all $I = f(\lambda)$ dependences $E_b = 300$ V/cm, $U_{mod} = 15$ V, $d_{mod} = 10$ kHz.

different photoresponse change rates and to define the corresponding scale parameters (and, respectively, the frequency ranges) using the wavelet spectrograms [9, 10]. In fact, a rather narrow frequency range of 9.5 to 10 kHz corresponding to the region of fast photocurrent variation and connected with the peak $\lambda = 862$ nm in the wavelength range 860÷865 nm was revealed in the wavelet spectrogram applying the Haar wavelet to the $I = f(\lambda)$ dependences (Fig. 1, curve *2*). Two other regions of fast photocurrent variation in the 830÷845 nm wavelength range (Fig. 1, curve *2*) that are in fact impossible to find out visually in this dependences, are clearly seen and localized in a wider (5 to 11 kHz) frequency range in the appropriate wavelet spectrogram.

The photocurrent spectrum rebuilding is a feature of the type $II_{\perp}$ second group samples as the strength variations of the external biasing field or its direction inversion. So, some peaks increase, while others decrease or disappear. This can be accompanied by appearance of new maxima, but already in other wavelength ranges. In this connection, it was of interest to study the spectral photocurrent dependences for the type $II_{\perp}$ samples under simultaneous biasing field and square-pulse modulating voltage of different polarity at the frequencies determined by wavelet spectra analysis and

corresponding to the peaks and regions of fast photocurrent variation. As it was expected, application of modulating field causes rebuilding of spectral dependences. So, the positive polarity square-pulsed voltage causes peaks in the 830÷ nm spectral range at 833 nm and 842 nm (Fig. 1, curve *1*), while the negative modulating voltage promotes the amplitude increasing of $\lambda = 862$ nm peak (Fig. 1, curve *3*) and appearance of low photosensitivity region in the 857÷860 nm range. The disappearance of long-wave maximum at $\lambda = 862$ nm and the appearance of a fast photocurrent variation region yet in the wavelength range is a feature of positive square pulses influence. All these facts are due obviously to changing of dominating photosensitivity bands at positive modulating voltage and suppression some of those at negative one.

It is noteworthy that the photocurrent fluctuations decrease at certain frequencies of square pulse voltage. In addition, new extremes appear in the spectra and reproducibility of the existing ones becomes improved. So, the 862 nm maximum is reproduced approximately in half of cases when the modulating voltage is absent while, in contrast, the fast photocurrent variation region is well observable. As the studies indicated, this extreme is reproduced stably only at negative modulating voltage and in the narrow frequency range of 9.3 to 10.4 kHz that practically corresponds to the above-mentioned range. In this case, the on-off time ratio of modulating pulses should be within limits of 10 to 20. For stable appearance of peaks at 833 nm and 842 nm, the frequency of positive polarity square pulses should be chosen within a wider range (5 to 10 kHz) that also corresponds to the above frequency range determined from the wavelet spectrograms. But in this case, it is just the on-off time ratio value that is of decisive importance and-should be of 18 to 20. As is seen, the reproducibility in some spectral ranges depends essentially on relation of additional modulating voltage parameters, namely, frequency and on-off time ratio. The time-frequency selectivity evidences obviously the interrelation between the processes of transport, accumulation, and recombination of nonequilibrium carries that define the interconsistent band rebuilding in the spectrum.

Note that the band rebuilding in the spectrum was observed before in the ZnSe crystals at the same experiment conditions, i.e. when E_b is parallel to the 2DSD boundaries. Therefore it is naturally to suggest that these features are caused mainly by some 2DSD aggregates. To verify this assumption, we have investigated $I = f(x)$ photocurrent dependences for the second group samples, where x is the narrow monochromatic probe coordinate on the sample surface (Fig. 2). The comparison of coordinate photocurrent dependences obtained during repeated scanning of the crystal surfaces at wavelengths corresponding to the photoresponse fast variation ranges allowed us to establish that the low reproducibility regions appear only on the $I = f(x)$ curves for the type $II_{\perp}$ samples (region with coordinates $x = 0.6 \div 2$ mm separated by dashed lines in the Fig. 2, curves *1* and *3*). These regions seem to include not only 2DSD but also other structure defects, for example, those appearing during the slip band formation. Those regions could cause the band rebuilding in the photocurrent spectrum under additional modulating field. Then the asymmetry of several extremes appearing at the biasing field inversion can be obviously connected with local redistribution of the contributions from complex photosensitivity centers. The consideration of the biasing field modulation with the pulse voltage con-

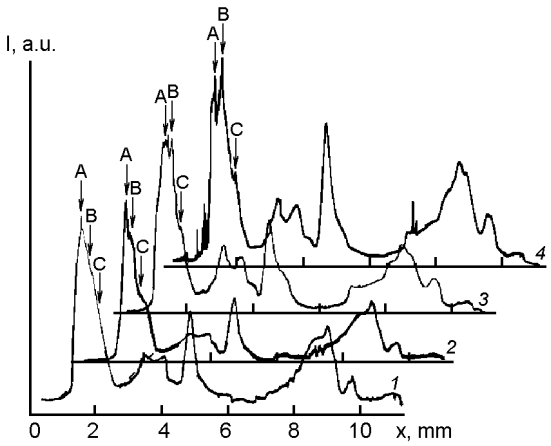

Fig. 2. Dependences $I = f(x)$ for the second-group $Cd_{0.9}Zn_{0.1}Te$ of $II_{\perp}$ type: under only bias field E_b, $\lambda = 862$ nm (*1*); under simultaneous influence of biasing field E_b and modulating negative square pulse voltage U_{mod} at on-off time ratio $n = 15$, scanned at $\lambda = 862$ nm (*2*); under only bias field E_b, scanned at $\lambda = 833$ nm (*3*); under simultaneous influence of biasing field E_b and modulating positive square pulse voltage U_{mod} at on-off time ratio $n = 20$, scanned at $\lambda = 833$ nm (*4*). For all $I = f(x)$ dependences $E_b = 300$ V/cm, $U_{mod} = 15$ V, $d_{mod} = 10$ kHz.

firms that suggestion. So, some extremes in the $I = f(x)$ dependences were rebuilt for the type $II_{\perp}$ samples whereas it was not found for the type $II_{\parallel}$ ones. In fact, it is seen from the presented $I = f(x)$ dependences for the type $II_{\perp}$ crystal (Fig. 2) that negative modulating square pulse voltage of 9.3 to 10.4 kHz frequency influences weakly the extreme A while suppressing strongly the B and C ones (Fig. 2, curve *2*). This explains the suppressed photosensitivity bands in long-wave region of the spectrum. However, positive polarity voltage of 5 to 10 kHz frequency influences causes an inverse effect, i.e., increasing the extreme A while practically not changing the extremes B and C. Thus, at the long-wave photoexcitation, it is just the extreme A that is dominant and obviously responsible for the photocurrent peak at $\lambda = 862$ nm. At the scanning of the crystal surface with monochromatic optical probe at 833 nm operating wavelength, the extremes A and B are substantially equal to one another (Fig. 2, curve *3*). The competition thereof seems to result in the appearance of a fast photocurrent variation region in the short-wave part of spectrum and to be not accompanied by appearance of additional peaks. While the positive pulse voltage stimulates the contribution of the maximum B and influences weakly the extremes A and C (Fig. 2, curve *4*) thus explaining the appearance of the peaks in the short-wave part of the spectrum, the negative voltage suppresses strongly all extremes and does not promote any essential transformation of $I = f(x)$ dependences. It follows that the additional electrical stimulation with positive square pulse voltage under the short-wave photoexcitation causes the domination of extreme B and thus promotes changing of the dominant photosensitivity bands in the PHC spectrum. It is seen that the coherent rebuilding of the photocurrent spectrum in the presence of additional square pulse voltage is caused by instability of certain regions that contain aggregates of 2DSD and other structure defects. This is confirmed also by simultaneous studies of the photocurrent spectra in the local regions of samples corresponding to the A, B, C maxima (Fig. 2) that were carried out using segmented contacts. In fact, the obtained photocurrent spectra are characterized by sharp narrow maxima and differ in λ_{max} values.

It is noteworthy that most samples under additional modulating voltage do not show the appearance or suppression separated peaks in the photocurrent dependences on the coordinate of monochromatic probe but only hardly visible changing of the photocurrent increase rates in certain regions. To discriminate visually such regions is often very difficult but due to possibility to show up local photoresponse features using wavelets [9, 10], those are well seen in the wavelet spectrograms of the studied $I = f(x)$ dependences for the $II_{\perp}$ samples. In addition, certain scale parameters (and, respectively, frequency ranges) corresponding to the regions of the fastest photocurrent variation in the $I = f(x)$ and $I = f(\lambda)$ dependences are similar to each other. The obtained experimental results point to the interrelation between sources of the spectral and spatial instabilities and their time and frequency selectivity indicates a possibility to reveal the structure defects aggregates of specific type and size. In addition, the consideration of the wavelet spectrograms obtained in the presence of modulating field and without it evidences other thinner influence features of two-dimensional and other types of structural defects aggregates on the photoelectric crystal properties that is subject of our further investigations.

Thus, in CdZnTe crystals, the spectral and spatial instabilities of photoresponse are interrelated. The simultaneous influence of the biasing and modulating fields has been found to cause rebuilding of the $I = f(x)$ and $I = f(\lambda)$ dependences which is accompanied by suppression or changing dominant photoconductivity bands taking place depending on the modulating voltage polarity. The comparison of spectral and coordinate photocurrent dependences and their wavelet spectrograms obtained at the appropriate polarity, frequency and on-off time ratio of modulating voltage makes it possible to reveal the interrelation between certain wavelength ranges of spectral instability and coordinates of structural defects aggregates that cause it. It is just the wavelet analysis of the dependences that provides the reliable determination of boundaries for the appropriate crystals regions that cause photoresponse instability in crystals.

This study was supported by the Fundamental Researches State Foundation of Ukraine.

References

1. P.Fougeres, P.Siffert, M.Hageali et al., *Nucl. Instr. and Meth. in Phys. Res.*, **428**, 38 (1999).

2. H.Hermon, M.Schieber, R.B.James et al., *Nucl.Instr.and Meth. in Phys. Res.*, **428**, 30 (1999).
3. V.K.Komar, V.P.Mygal, S.V.Sulima, A.S.Phomin, *Fiz.i Tekhn.Polupr.*, **40(2)**, 133 (2006).
4. I.A.Klimenko, V.P.Mygal, *Semiconductors*, **36(4)**, 375 (2002).
5. V.Komar, A.Gektin, D.Nalivaiko et al., *Nucl. Instr.and Meth. in Phys.Res.*, **458(1–2)**, 113 (2001).
6. V.A.Vasil'ev, *Technology and Engineering in Electronics*, **2**, 46 (2002).
7. I.G.Gavrikova, V.P.Mygal, A.L.Rvachev, R.V.Chigarkova, *Izv.VUZov:Fizika*, **10**, 134 (1976).
8. V.K.Komar, V.P.Mygal, O.N.Chugai et al., *Appl.Phys.Lett.*, **81**, 4195 (2002).
9. N.M.Astaf'eva, *Usp.Fiz.Nauk*, **166**, 1145 (1996).
10. I.M.Dremin, O.V.Ivanov, V.A.Nechitailo, *Usp. Fiz.Nauk*, **171, 465 (2001).**

Електроіндуковані спектральна та просторова нестійкості фотовідгуку кристалів CdZnTe

В.П.Мигаль, О.С.Фомін

Виявлено і досліджено особливості залежностей $I = f(\lambda)$ та $I = f(x)$ для кристалів $Cd_{1-x}Zn_xTe$, що містять двовимірні дефекти структури, які виявляються при одночасній дії зміщувального та модулювального полів. На основі зіставлення спектральних і координатних залежностей фотоструму та їх вейвлет-спектрограм, одержаних при відповідних полярності, частоті та відносній тривалості прямокутних імпульсів модулювальної напруги, встановлено зв'язок між певними діапазонами довжин хвиль спектральної нестійкості та координатами ансамблів дефектів структури, що їх породжують.